Reductive C–O Silylation by Rhodium/Lanthanum Cooperative Catalysis

Authors: Rin Seki,[1] Hikaru Takaya,*[2,3] and Yoshiaki Nakao*[1]

Affiliations:

1 *Department of Material Chemistry, Graduate School of Engineering, Kyoto University, Nishikyo-ku, Kyoto 615-8510, Japan*

2 *Department of Life Science, Faculty of Life & Environmental Sciences, Teikyo University of Science, Main Buld #15-05, 2-2-1 Senjyusakuragi, Adachi-ku, Tokyo 120-0045, Japan*

3 *Division of Photo-Molecular Science, Institute for Molecular Science, Myodaiji, Okazaki, Aichi 444-8585, Japan*

*Corresponding author.

Email: takayahikaru@ntu.ac.jp, nakao.yoshiaki.8n@kyoto-u.ac.jp

Abstract: In the realm of synthetic organic chemistry, a transformation enabling access to high-value-added compounds from readily available starting materials is the most ideal. Cross-electrophile coupling (XEC) reactions, the coupling of two different electrophiles, are of great importance in terms of the variety and availability of electrophiles compared with common nucleophiles. Among various electrophiles, phenols and aryl ethers can be particularly useful aryl electrophiles owing to their low toxicity, robustness, and availability. However, XEC of phenols and aryl ethers remains elusive because it is generally challenging to distinguish between two electrophiles and selectively obtain cross-coupling products under harsh reaction conditions that are often required for the activation of the less reactive C–O bonds. Meanwhile, chlorosilanes are easily available and serve as silicon electrophiles to access the most known organosilicon compounds through coupling with organic nucleophiles. Considering the utility of organosilicon compounds as organic materials and building blocks for organic synthesis, the XEC of phenols and chlorosilanes can be a highly practical and useful transformation but has never been viable. Here we describe the XEC of phenol and alcohol derivatives with chlorosilanes by cooperative rhodium and lanthanum catalysis. This reaction allows a range of anisole derivatives as well as benzylic ethers, phenols, benzylic alcohols, allylic ethers, and allylic alcohols to be transformed into various organosilicon compounds in a single step. Mechanistic studies including kinetics, stoichiometric organometallic reactions, XAS, and theoretical calculations suggest a heterobimetallic complex bearing a Rh–Mg and/or Rh–La bond as a key catalytically active species. This method can be applied to the development of novel silicon-containing organic materials and drugs containing silicon as a carbon isostere. On the other hand, the XEC of phenol derivatives enables the use of biomass-derived resources as an alternative to petroleum to produce useful compounds in a sustainable manner.

Main Text

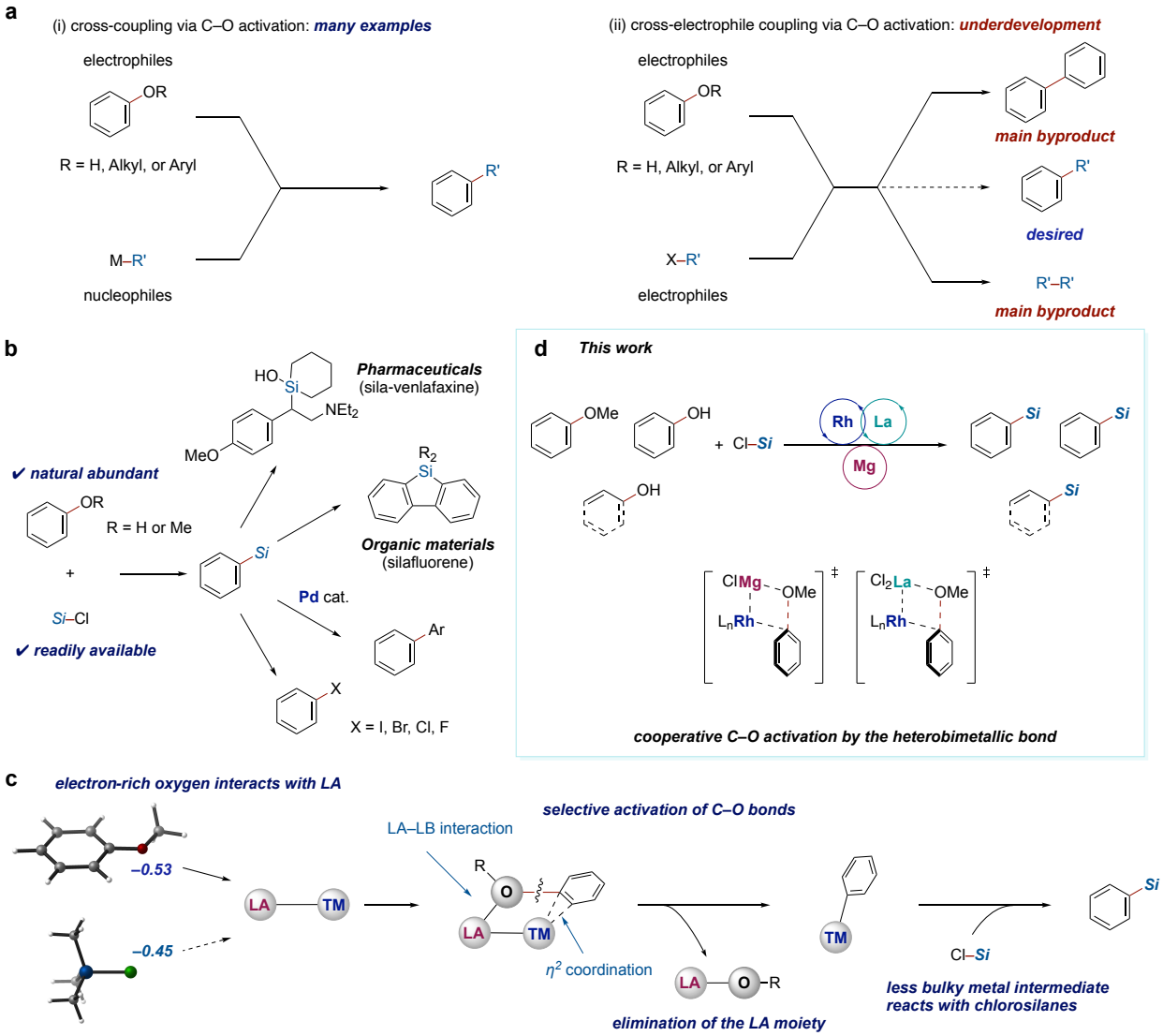

Fig. 1. Background of C–O activation. (**a**) Difficulty in XEC of phenol or aryl ether derivatives. (**b**) The utility of reductive C–O silylation. (**c**) Our strategy for achieving XEC of phenol derivatives. (**d**) This work: reductive C–O silylation of alcohol derivatives by the cooperative action of Rh, La, and Mg.

Cross-electrophile coupling (XEC) reactions have significant advantages over conventional nucleophile–electrophile cross-coupling reactions in terms of the availability and chemical stability of common organic electrophiles as starting materials.[1,2] Electrophiles are often employed as precursors of common nucleophilic reagents and can be more readily available than carbon nucleophiles. In addition, electrophiles, being organic compounds, exhibit superior chemical stability in comparison to nucleophiles in case they possess carbon–metal bonds. Among various electrophiles, phenols and aryl ethers can be useful due to their low toxicity, robustness, and availability.[3] These compounds can be derived from ubiquitous biomass and are sustainable alternatives to petroleum-based chemical feedstocks.[4] However, the XEC of phenols or aryl ethers remains elusive, probably owing to the intricate challenge of discriminating between two electrophiles and accessing cross-

coupling products selectively, under harsh conditions that are often required for the activation of the C–O bonds (Fig.1a).

Chlorosilanes are byproducts of the Müller-Rochow process[5] and have been utilized as raw materials in the chemical process of common organosilicon compounds starting from hydrosilanes and disilanes,[6,7,8] which are further transformed into organosilicon products including organic materials[9] such as siloles and silafluorenes[10] and biologically active molecules in which silicon serve as a carbon isostere to improve pharmacological activity.[11,12] Organosilicon compounds are also versatile building blocks to perform several useful synthetic transformations such as the Hiyama-coupling,[13,14] halogenation,[15,16] and the Hosomi–Sakurai reaction.[17,18] Accordingly, the XEC reaction of phenol and alcohol derivatives with chlorosilanes can be an ideal transformation to produce organosilicon compounds in an efficient and sustainable manner (Fig.1b).

The XEC of phenols and aryl ethers with chlorosilanes has remained highly challenging[3,19,20,21] due probably to the poor cross-selectivity. XEC using inherently less reactive substrates often give more homocoupling products derived from more reactive coupling partners.[1] Reductive homo-coupling reactions of naphthyl ethers and benzyl ethers have been reported, but the XEC of aryl ethers and phenols has been unexplored.[22,23,24] The only reported example of the XEC of aryl ethers requires a directing group[25] to compensate for the much poorer reactivity of the Ar–O bonds than that of Ar–halogen bonds.[26] The XEC of chlorosilanes were recently reported in 2020[27] and 2022,[28] however, these reactions necessitated the use of reactive aryl triflates.[3]

To circumvent these issues, we have focused on the use of transition metal/Lewis acidic metal heterobimetallic catalysis. Our previous work demonstrated that heterobimetallic complexes could cleave strong σ-bonds, triggered by Lewis acid–base interactions.[29] We have hypothesized that anisole could react with a bimetallic catalyst in preference to chlorosilanes due to the possibly greater Lewis basicity of O than Cl (calculated NBO charges[30]: O in anisole = –0.53; Cl in chlorotrimethylsilane = –0.45) (Fig.1c). Sterically demanding chlorosilanes could be inaccessible to the crowded catalyst sites composed of two metal centers coordinated by supporting ligands. Heterobimetallic catalysts bearing a Lewis acidic site being able to dissociate from the transition metal center upon the Ar–O bond activation could then allow chlorosilanes to access the transition metal center easily, enabling the desired cross-selectivity.

Herein, we report the reductive cross-coupling of phenol derivatives and chlorosilanes catalyzed cooperatively by rhodium and lanthanum using magnesium powder as a stoichiometric reductant. This reaction allows a selective XEC reaction of chlorosilanes with not only anisole derivatives but also benzylic ethers, phenols, benzylic alcohols, allylic ethers, and allylic alcohols to afford various functional organosilicon compounds in a single operation starting from the abundant chemical feedstocks. Mechanistic studies including kinetics, stoichiometric organometallic reactions,

XAS, and theoretical calculations indicate that heterobimetallic complexes bearing Rh–Mg and/or Rh–La bonds are responsible for the selective and cooperative C–O and Si–Cl bond functionalization (Fig.1d).

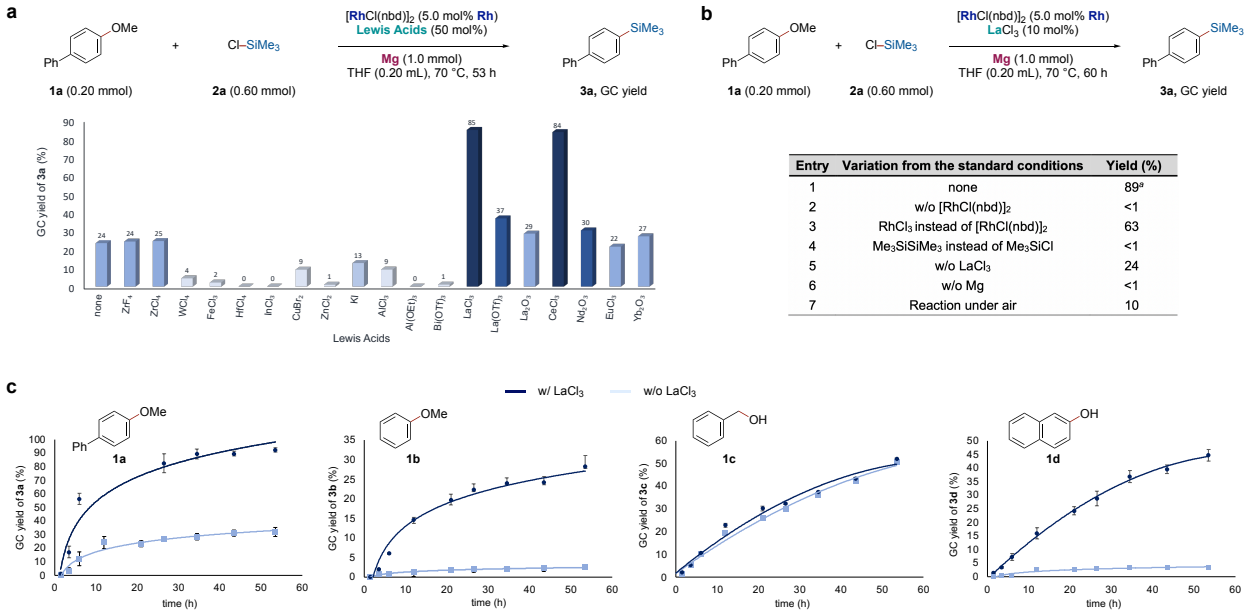

Fig. 2. Reaction conditions optimizations. (**a**) Lewis acids screening. (**b**) Control experiments. (**c**) Time-course studies with four substrates with or without $LaCl_3$. [a] The reaction was run on a 0.60 mmol scale.

First, we tested the reaction of 4-methoxybiphenyl (**1a**) and chlorotrimethylsilane (**2a**) with a catalytic amount of $[RhCl(nbd)]_2$ and a Mg reductant. After 53 h at 70 °C, we obtained demethoxysilylated product **3a** in 24% yield. To improve the yield, we investigated the effects of Lewis acidic metal co-catalysts, and $LaCl_3$ showed the highest catalytic activity, affording **3a** in 85% yield (Fig. 2a). $CeCl_3$, which has a resemble chemical property to La, also showed similar activity. We also conducted some control experiments (Fig. 2b). As we expected, **3a** was not obtained in the absence of a Rh catalyst and Mg powder. When we used $(Me_3Si)_2$ instead of Me_3SiCl, **3a** was not observed, indicating this reaction did not proceed through the formation of disilanes.[31] $RhCl_3$ also catalyzed the transformation, and no particular ligands were found necessary. We also optimized temperatures and solvents to run the reaction at 70 °C in THF giving the best results. To evaluate the importance of $LaCl_3$, we examined the reaction of four different substrates, including **1a**, anisole (**1b**), benzyl alcohol (**1c**), and 2-naphthol (**1d**), in the presence or absence of $LaCl_3$. In each case, $LaCl_3$ showed a dramatic acceleration of the reaction to improve the reaction rates and product yields, except for benzyl alcohol which was equally reactive under both conditions (Fig. 2c).

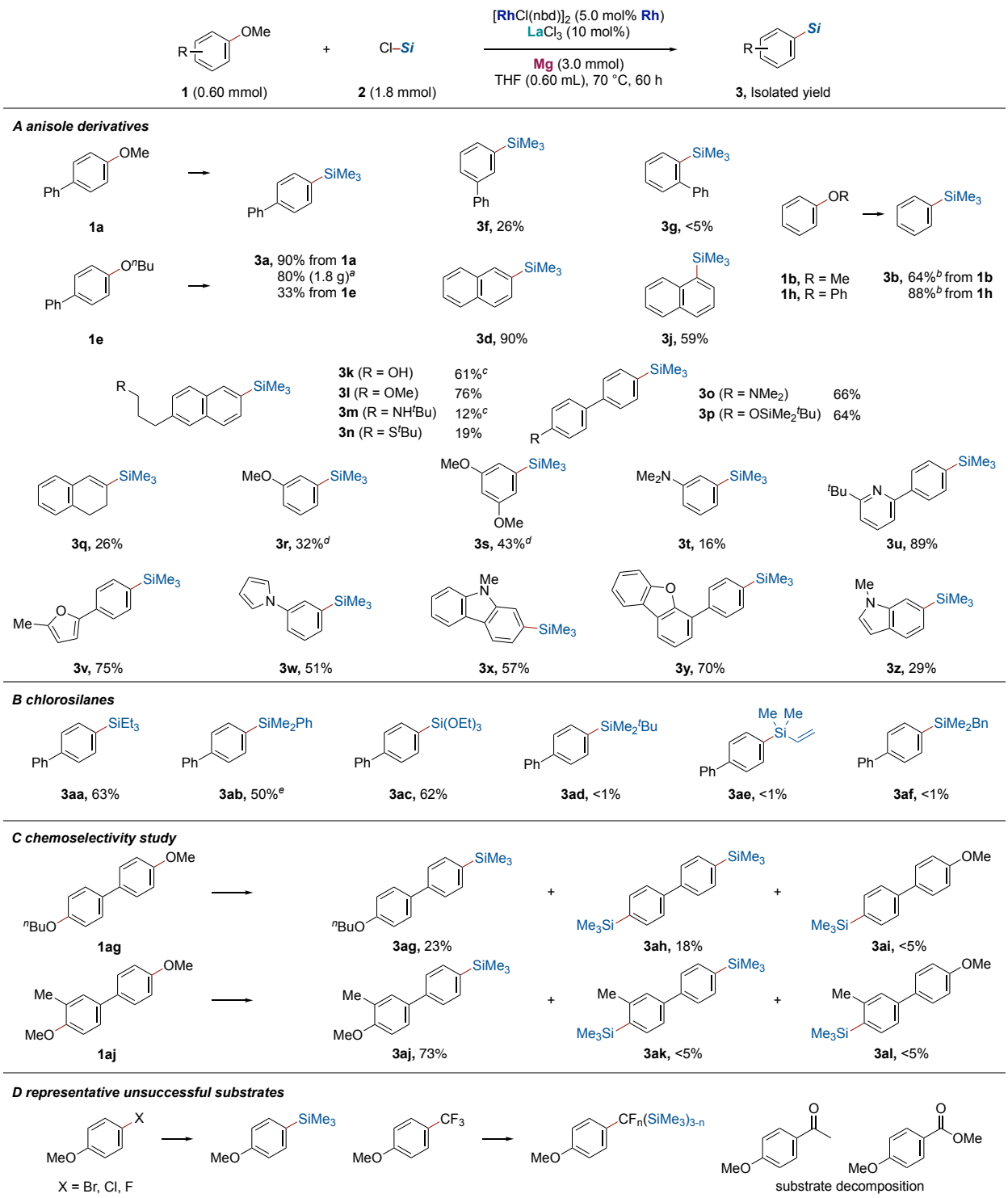

Fig. 3. Substrate scope of anisole derivatives. Standard reaction conditions: anisole derivatives (0.60 mmol) and chlorosilanes (1.8 mmol) with $[RhCl(nbd)]_2$ (5.0 mol% Rh), $LaCl_3$ (10 mol%), and Mg (3.0 mmol) in THF (0.60 mL) at 70 °C for 60 h. [a] A gram-scale reaction using **1a** (10 mmol), **2a** (30 mmol), $RhCl_3$ (5.0 mol%), $LaCl_3$ (10 mol%), and Mg (30 mmol) in THF (10 mL) at 70 °C for 60 h. [b] GC yield determined using $C_{12}H_{26}$ as the internal standard. [c] 2.4 mmol of **2a** was used. [d] 2.4 mmol of **2a** was used. After 3 days and then 5 days, **2a** (1.8 mmol x 2) was further added. The reaction was run for a total of 7 days. [e] The reaction was run at 120 °C.

With the optimal conditions in hand, we investigated the scope of substrates (Fig. 3A). The reaction of **1a** afforded **3a** in good yields both on 0.60 mmol and 10 mmol scales, demonstrating the scalability of this reaction. However, 4-butoxybiphenyl (**1e**) and 3-methoxybiphenyl (**1f**) showed attenuated reactivity and 2-methoxybiphenyl (**1g**) didn't react. These results indicate that this catalyst system is sensitive to the steric environment of the reaction site. The protocol was also applicable to **1b**, diphenyl ether (**1h**), and naphthyl methyl ethers (**1i**, **1j**). Functional groups such as alcohol (**1k**), dialkyl ether (**1l**), secondary amine (**1m**), thioether (**1n**), arylamine (**1o**), and silyl-protected phenolic OH (**1p**) were compatible under the reaction conditions to give **3k**–**3p**. The primary alcohol was protected by chlorosilanes *in situ* and did not hamper the progress of the intended Ar–O silylation. Conversely, sterically hindered secondary amine was not protected completely, furnishing unwanted C–O hydrogenated products due presumably to the presence of the free NH group. The poor yield of **3n** was caused by competitive and undesired alkyl–S bond activation and silylation. Vinyl ether (**1q**) also provided corresponding organosilicon compound **3q** albeit in low yield. Multi-methoxy benzene derivatives (**1r**, **1s**) and *m*-dimethylaminoanisole (**1t**) underwent silylation in moderate yields. We could also introduce the trimethylsilyl moiety to a range of heterocycles such as pyridine (**3u**), furan (**3v**), pyrrole (**3w**), carbazole (**3x**), dibenzofuran (**3y**), and indole (**3z**). Different chlorosilanes were also investigated to see triethylsilyl- (**3aa**), dimethylphenylsilyl- (**3ab**), and triethoxysilyl- (**3ac**) moieties were successfully introduced, whereas *tert*-butyldimethylsilyl-, vinyldimethylsilyl-, and benzyldimethylsilyl- groups were unable to be installed (**3ad**–**3af**) (Fig. 3B). The reactions of **1e**, **1f**, and **1g** show that the catalyst system is quite sensitive towards steric factors at the vicinity of the reacting C–O bonds. In other words, our catalyst can distinguish a slight steric difference and selectively cleave less hindered C–O bonds. Intrigued by this, we examined the reactions of substrates bearing multiple C–O bonds to evaluate the chemoselectivity of this reaction (Fig. 3C). The methoxy moiety of **1ag** was preferentially silylated over the butoxy moiety, demonstrating the sterically controlled chemoselectivity. The *ortho*-methyl of **1aj** hampered the Ar–OMe cleavage and the less hindered site was selectively silylated to give **3aj**. Fig. 3D showed representative unsuccessful substrates. Dehalogenation and silylation proceeded in the case of 4-bromo-, 4-chloro-, and 4-fluoroanisole, respectively.[32] In addition, a benzyl–F bond was also cleaved and silylated. Although we did not focus on organic halides in this study, their XEC with chlorosilanes remains elusive and may be possible with this catalytic system. Substrates containing carbonyl moiety were decomposed and gave complex mixtures.

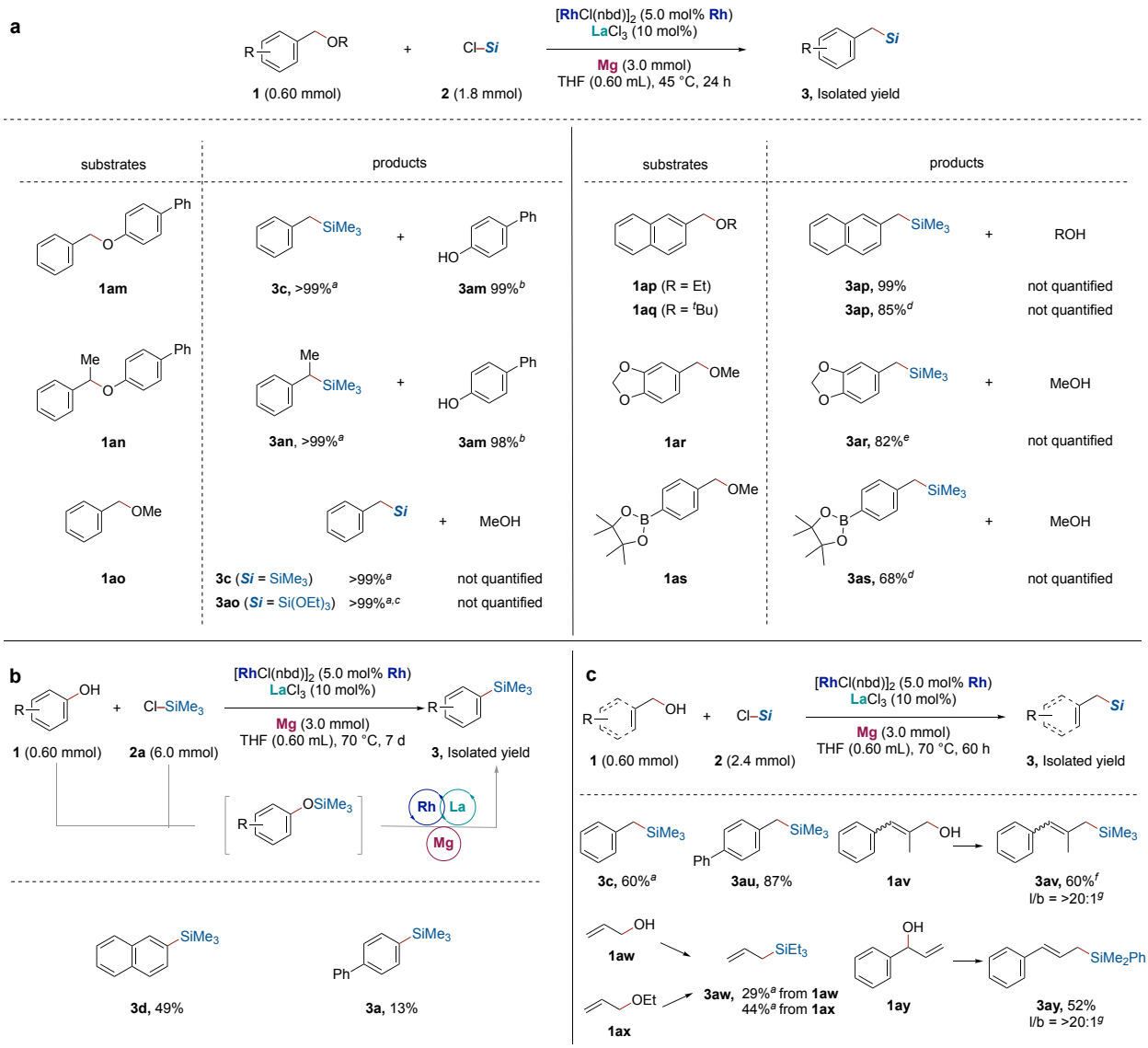

Fig. 4. Scope of benzyl ethers, arenols, allylic ethers, and allylic alcohols. (**a**) Reductive Bn–O silylation, standard reaction conditions: benzyl ether derivatives (0.60 mmol), chlorosilanes (1.8 mmol), $[RhCl(nbd)]_2$ (5.0 mol% Rh), $LaCl_3$ (10 mol%), and Mg (3.0 mmol) in THF (0.60 mL) at 45 °C for 24 h. (**b**) Reductive Ar–OH silylation, standard reaction conditions: phenol derivatives (0.60 mmol), **2a** (2.4 mmol), $[RhCl(nbd)]_2$ (5.0 mol% Rh), $LaCl_3$ (10 mol%), and Mg (3.0 mmol) in THF (0.60 mL) at 70 °C for 7 days. After 3 days and 5 days, **2a** (1.8 mmol x 2) was added. (**c**) Reductive Bn/Allyl–OH silylation, standard reaction conditions: alcohol derivatives (0.60 mmol), chlorosilanes (2.4 mmol), $[RhCl(nbd)]_2$ (5.0 mol% Rh), $LaCl_3$ (10 mol%), and Mg (3.0 mmol) in THF (0.60 mL) at 70 °C for 60 h. [a] GC yield determined using $C_{12}H_{26}$ as the internal standard. [b] **3am** were detected after quenching by saturated NH_4Cl aqueous solution. [c] The reaction was run at room temperature. [d] The reaction was run at 70 °C for 60 h. [e] The reaction was run at room temperature for 60 h. [f] The reaction was run at room temperature for 12 h. [g] Liner/branch selectivity was determined by ^1H NMR.

We questioned whether the bimetallic catalysis could also functionalize other types of C–O bonds. Both primary (**1am**) and secondary benzyl aryl ethers (**1an**) were smoothly silylated quantitatively. A type of *O*-substituent was not important for the benzyl–O activation. Methyl benzyl ether (**1ao**), ethyl benzyl ether (**1ap**), and sterically demanding *tert*-butyl benzyl ether (**1aq**) all

reacted. Dioxolane moiety (**1ar**) and boryl functionality (**1as**) were tolerated in this system (Fig. 4a). In terms of availability, alcohols are more abundant substrates compared with corresponding ethers. However, since O–H bonds are generally weaker than C–O bonds in alcohol, the C–O bond cleavage of alcohol has been highly challenging.[3,33,34] Under slightly modified conditions, the direct silylation of 2-naphthol and 4-phenylphenol afforded the corresponding products **3d** and **3a**, albeit in low to moderate yield (Fig. 4b). It is highly likely that the C–O bond cleavage proceeds after silyl ether formation by the reaction of chlorosilane and phenol. We also succeeded in the activation of benzyl alcohols to give **3c** and **3au**. Allylic alcohols/ethers were also silylated under the same conditions, giving corresponding products **3av**, **3aw**, and **3ay**. In the reaction of 2-methyl-3-phenylprop-2-en-1-ol (**1av**) and 1-phenylprop-2-en-1-ol (**1ay**), we found exclusive linear selectivity (Fig. 4c).

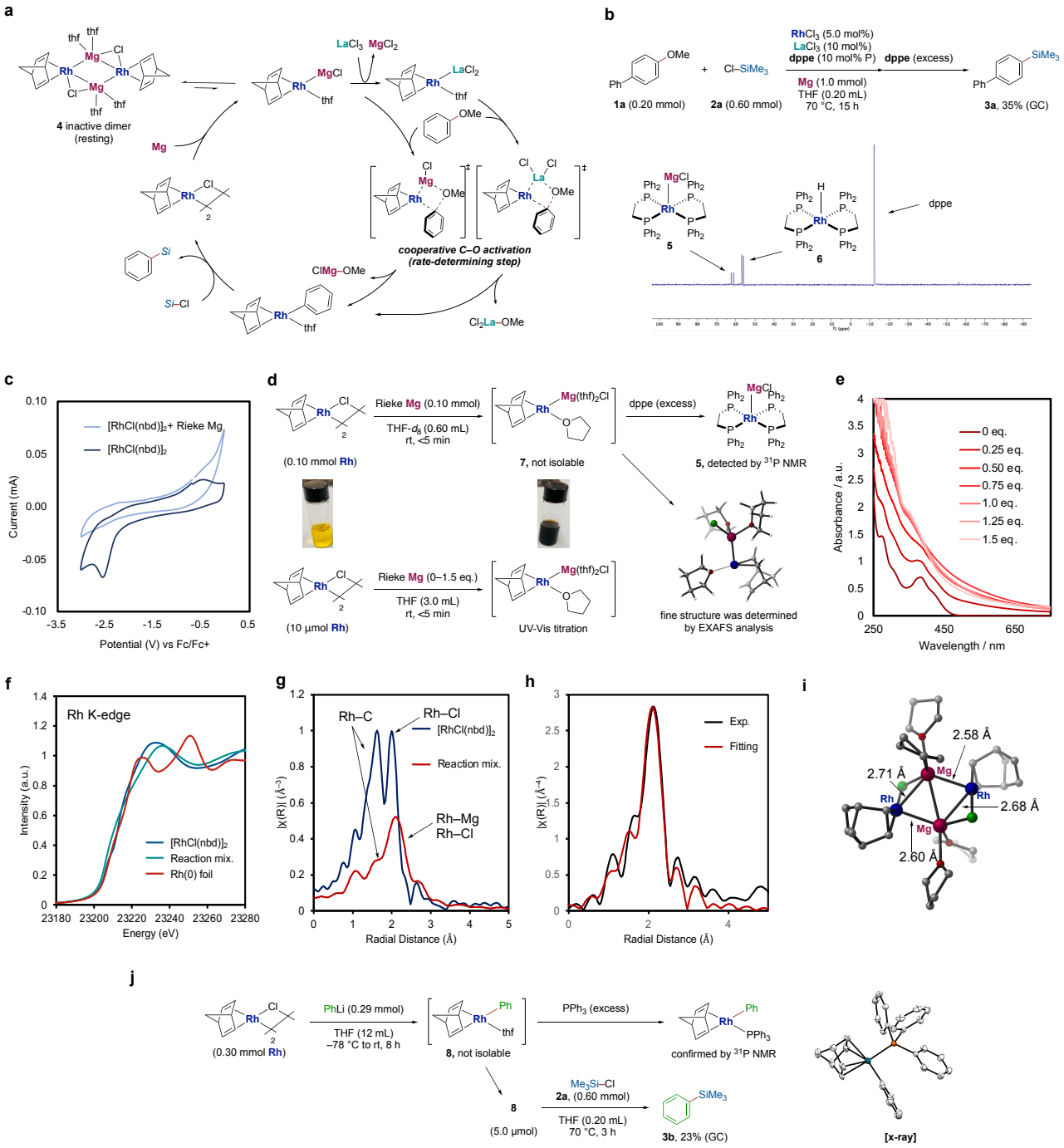

Fig. 5. Mechanistic studies. (**a**) Plausible reaction mechanism. (**b**) Resting state trapping experiment using phosphine ligand. (**c**) Cyclic voltammetry. (**d**) The stoichiometric reaction of $[RhCl(nbd)]_2$ with Rieke Mg. (**e**) UV-Vis titration of $[RhCl(nbd)]_2$ with Rieke Mg. (**f–h**) XAS analysis for Rh K-edge. (**i**) Fitted structure of **4**. (**j**) Stoichiometric reaction of $[RhCl(nbd)]_2$ with phenyllithium and **2a**.

A plausible catalytic cycle of this reaction is suggested in Fig. 5a. First, the Rh precursor reacts with Mg to generate the Rh–Mg heterobimetallic complex. Under the conditions without $LaCl_3$, the C–O bond is cleaved by the Rh–Mg complex. In the presence of $LaCl_3$, the Rh–La heterobimetallic complex could also be generated via the transmetalation between the Rh–Mg complex and $LaCl_3$. According to mechanistic studies (*vide infra*), the heterobimetallic Rh–Mg and Rh–La complexes are

considered to have covalent-like coordination (X-type) of Mg and La to Rh.[35,36] We assume a cooperative activation mode similar to our previous study with the Rh–Al complexes,[29] that is, the oxygen of aryl ethers coordinates to the Lewis acidic center, which is Mg or La in this study, and the C–O bond is cleaved by the electron-rich Rh center to give an arylrhodium(I) intermediate. In this activation mode, Lewis acidic metals play dual roles: they form Lewis pairs with the substrate to weaken strongly polarized σ-bonds, while they render the transition metal center electron-richer by their strong σ-donating properties. In addition, as mentioned in the introduction, this activation mode would also contribute to the cross-selectivity by favoring the coordination of the ethereal oxygen, which would have higher Lewis basicity over chlorosilanes. Then, the arylrhodium(I) intermediate reacts with chlorosilane to yield target arylsilanes and regenerate active bimetallic species.

To gain some evidence to support the plausible reaction mechanism, we conducted a series of experimental and theoretical mechanistic studies. First, to identify a resting rhodium complex, we added 1,2-bis(diphenylphosphino)ethane (dppe) to the reaction mixture both before and after the reaction and analyzed them by ^{31}P NMR spectroscopy. $(Dppe)_2RhMgCl$ (**5**) and $(dppe)_2RhH$ (**6**) complexes, reported by Bogdanović and Leitner *et al.*,[37] were detected after the reaction, indicating the suggested Rh–Mg heterobimetallic species (Fig. 5b). This was presumably generated through the reduction of the Rh(I) complex by Mg powder and should bear a highly electron-rich Rh center. Through cyclic voltammetry (CV) analyses, the reduction peak of the Rh(I) complex was recorded at around –2.5 V vs. Fc/Fc^+ and disappeared upon treatment with Mg, an observation consistent with our hypothesis (Fig. 5c). Although we failed to isolate the Rh–Mg heterobimetallic species due to its low stability, we verified the generation of the Rh–Mg heterobimetallic bond through a stoichiometric reaction of $[RhCl(nbd)]_2$ with Mg under the same conditions (Fig. 5d). We found that just equimolar Mg reacted with the Rh complex through titration using an ultraviolet-visible (UV-Vis) spectrometer (Fig. 5e). From these observations, a complex containing a Rh–Mg bond would likely be a resting state. Unfortunately, ^{1}H NMR spectroscopy did not provide useful information due to the contamination of open-shell by-products. We also performed various experiments to exclude possible heterogeneous catalysis (see SI).[38]

We then conducted X-ray absorption spectroscopy (XAS) analyses to elucidate the fine structure and the electronic character of the resting Rh–Mg complex. We performed Rh K-edge XAS measurements of the reaction mixtures and several standard samples. The X-ray absorption near edge structure (XANES) measurements showed the active species should bear a Rh center with a highly reduced valence equal to or greater than Rh(0) foil (Fig. 5f). From extended X-ray absorption fine structure (EXAFS) obtained from the reaction mixture and $[RhCl(nbd)]_2$ exhibits that the scattering at 1.5 Å corresponding to the Rh–nbd coordination is still present in the reaction mixture (Fig. 5g).[39,40] The decreased peak intensity associated with the Rh–C moiety in the reaction mixture compared with that in starting $[RhCl(nbd)]_2$ showed one of the olefin ligands dissociated from the Rh center upon reacting with Mg. The substantially higher shift with reduced intensity of the Rh–Cl scattering (2.0 Å) supports the formation of the proposed catalytic intermediate **4** bearing Rh–Cl–Mg linkage resulting from the Cl ligand recombination. To estimate the entire structure by EXAFS, we calculated

some possible structures by density functional theory (DFT) at the level of B3LYP/LANL2DZ-6-31+g(d) and extracted atomic coordinates for FEFF fitting analysis. For the reaction mixture, Rh dimer complex **4** containing the Rh–Mg heterobimetallic bond and the experimentally obtained spectra showed perfect coincidence in curve fitting (Fig. 5h) with a good *R*-factor (0.0139) and reasonable other parameters (see SI). In the optimized structure of **4**, two Rh and Mg atoms formed a square geometry, containing two longer (2.68 and 2.71 Å) and two shorter (2.58 and 2.60 Å) Rh–Mg heterobimetallic bonds (Fig. 5i). Shorter bonds are within the sum of covalent radii, which is expected to behave as X-type heterobimetallic bonds. The EXAFS spectrum of the stoichiometric reaction was also fitted in a similar manner and completely matched with another monomeric Rh–Mg heterobimetallic complex **7** (see SI).

To investigate the C–Si bond formation steps, we examined stoichiometric reactions using phenylrhodium(I) complexes and **2a** (Fig. 5j). According to the literature,[41] the reaction of $[RhCl(nbd)]_2$ with phenyllithium afforded phenylrhodium(I) complex **8** possibly, which could not be fully characterized due to its low stability. Its treatment with triphenylphosphine, however, successfully gave $(nbd)(PPh_3)RhPh$, which could be identified by X-ray single crystal structure analysis. The reaction of **8** with **2a** in THF indeed afforded **3b** albeit in low yield, indicating that Mg was not involved in the C–Si bond formation step. In addition, it was stated that the reaction of chlorosilane with magnesium does not produce the silicon Grignard reagent in a previous study.[42] Considering these facts, we conclude that chlorosilane acts as an electrophile in this reaction.

We then carried out a series of kinetic studies and estimated the reaction rate equation as shown below.

$$v = k[\mathbf{Rh}]^{0.5}[\mathbf{La}]^{0.5}[\mathbf{1}\boldsymbol{a}]^{0.5}[\mathbf{2}\boldsymbol{a}]^{0}$$

The reaction rate depending on [**1a**] would indicate that the C–O bond cleavage step can be rate-determining. Regarding its 0.5th−order dependence, we discuss some possible rationale in the supporting information. Both Rh and La also play some roles in the rate-determining step, where **2a** should not be involved. These results would support our hypothesis that the C–O bond is activated cooperatively by the Rh–La heterobimetallic complex. We assume that the Rh–Mg species exists mainly as an inactive dimer, which is in equilibrium with a reactive monomer species, as can be supported by the 0.5th-order dependence on [Rh]. A similar inactive Rh–La dimer may also exist in an equilibrium manner to be supported by the observed 0.5th-order dependence on [La].

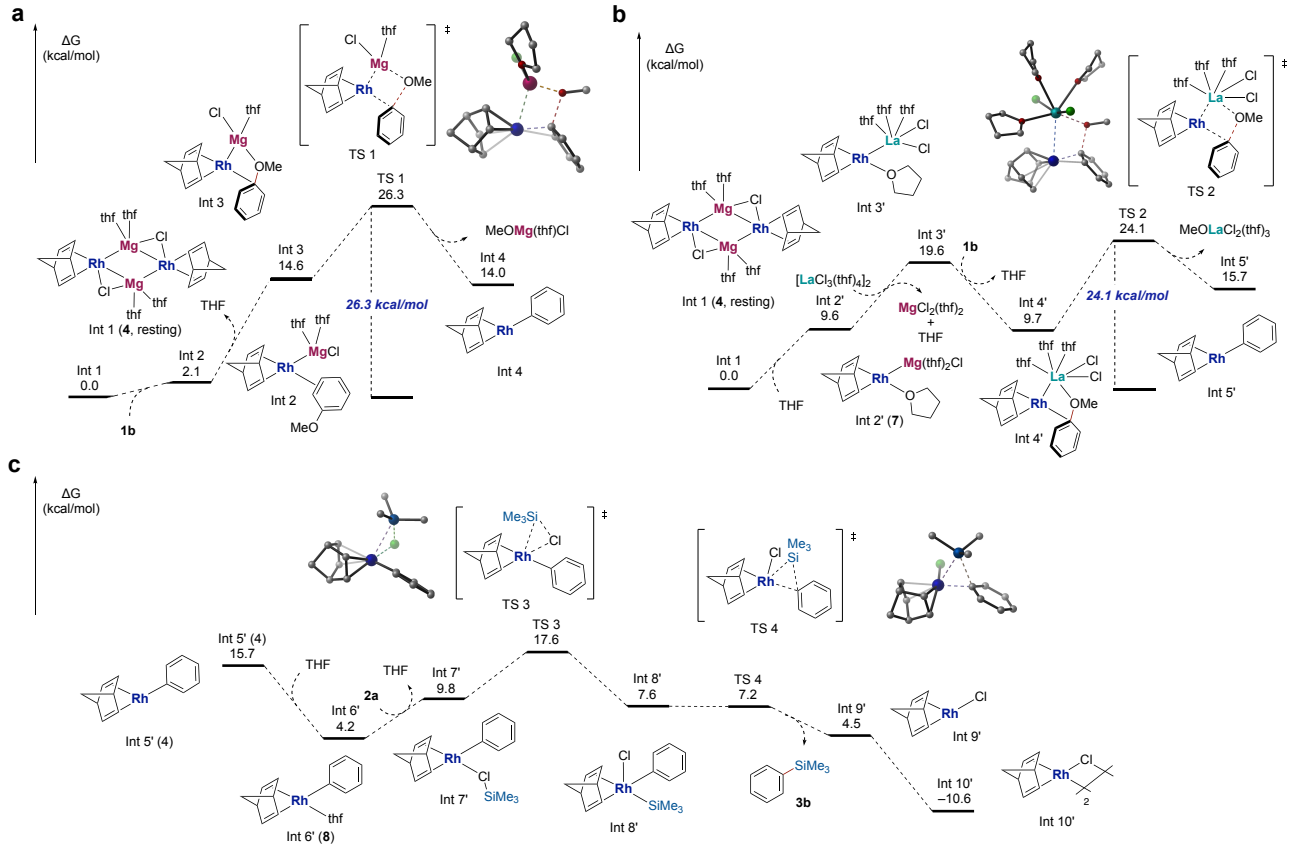

Fig. 6. Theoretical calculations. Density functional theory (DFT) calculations were conducted as follows: M06/LANL2TZ-6-311++g(d,p)/SMD(THF)//B3LYP/LANL2DZ-6-31+g(d) level of theory. (**a**) C–O bond activation by Rh–Mg heterobimetallic complexes. (**b**) C–O bond activation by Rh–La heterobimetallic complexes. (**c**) Oxidative addition of Si–Cl bond and reductive elimination of C–Si bond.

For a deeper understanding, we carried out the DFT calculations for the whole catalytic process with **1b** as a model substrate (Fig. 6). The calculations have suggested two possible pathways for the C–O bond activation in a cooperative manner by either Rh–Mg or Rh–La heterobimetallic complexes. The Rh–Mg inactive dimer complex bearing norbornadiene as a ligand can readily generate the active Rh–Mg monomer upon coordination of **1b**. The C–O activation proceeds with an activation barrier reasonable for the reaction progress at 70 °C ($\Delta G^{\ddagger}$ = 26.3 kcal/mol). From kinetic studies, $LaCl_3$ would also play a significant role in the C–O bond activation step. In this context, we would hypothesize that an active species for the C–O bond activation could also be the Rh–La heterobimetallic complex generated through transmetalation between Rh–Mg and $LaCl_3$, which could be feasible according to the calculations. The cooperative C–O bond activation by the Rh–La complex needs indeed lower activation energy ($\Delta G^{\ddagger}$ = 24.1 kcal/mol) compared with that by the Rh–Mg complex. These C–O bond activation pathways in any case are likely endergonic (ΔG = +14.0/+15.7 kcal/mol), as can be supported by experimental results (see SI), to give the norbornadiene-coordinated phenylrhodium(I) complex and Mg–OMe and/or La–OMe species. The phenylrhodium(I) complex then reacts with **2a** to afford arylsilane product **3b** through oxidative addition of the Cl–Si bond to the rhodium center followed by C–Si bond-forming reductive elimination to regenerate the chlororhodium(I) species in an exergonic manner overall.

In summary, we have achieved reductive silylation via the activation of inherent unreactive C–O bonds by rhodium/lanthanum cooperative catalysis. This transformation can be characterized by its versatility to allow different types of C–O bonds including both C–OMe and C–OH bonds at aryl, benzylic, and allylic positions in the presence of some functional groups to cover a wide range of substrates. Mechanistic studies have suggested that highly reactive heterobimetallic complexes should be catalytically generated by just mixing commercially available rhodium, lanthanum, and magnesium reagents and responsible for the high reactivity towards the activation/functionalization of the inactivated C–O bonds. The reaction developed herein would provide a novel and practical way to access novel organosilicon compounds and accelerate further studies on the reactivity of the heterobimetallic intermediates for useful catalytic transformations, such as valorization of naturally occurring polymers including lignin, through activation of C–O and other less reactive bonds.

Data availability

Crystallographic data for the structures reported in this article have been deposited at the Cambridge Crystallographic Data Centre, under deposition number 2243914. Copies of the data can be obtained free of charge via https://www.ccdc.cam.ac.uk/structures/. All other data supporting the findings of this study are available within the Article and its Supplementary Information, or from the corresponding author upon reasonable request.

Acknowledgments:

We thank Dr. Kentaro Teramura (Kyoto University), Dr. Soichi Kikkawa (Tokyo Metropolitan University), and Dr. Seiji Yamazoe (Tokyo Metropolitan University) for the X-ray absorption spectroscopy. We thank Dr. Kazuhiko Semba (Kyoto University) for the X-ray crystallographic analysis. The synchrotron XAS measurements were carried out at SPring-8 beamline of BL01A1 or BL14B2 (2022A1627 and 2022B1763). We thank Dr. Daiki Shimizu (Kyoto University) for the discussion about electron paramagnetic resonance and cyclic voltammetry measurements.

Funding:

This work was supported by JSPS KAKENHI Grant JP20H00376. R.S. is grateful for Research Fellowships from the Japan Society for the Promotion of Science (JSPS) for Young Scientists.

Author contributions:

Y.N. directed the research. R.S., H.T., and Y.N. designed the overall project. R.S. conducted all experiments, analyses, and density functional theory calculations. R.S. and H.T. conducted XAS experiments and curve-fitting. R.S., H.T., and Y.N. prepared the manuscript.

Competing interests: The authors declare no competing interests.

References and Notes

1. Everson, D. A. & Weix, D. J. Cross-electrophile coupling: principles of reactivity and selectivity. *J. Org. Chem.* **79**, 4793–4798 (2014).

2. Ackerman, L. K. G., Lovell, M. M. & Weix, D. J. Multimetallic catalysed cross-coupling of aryl bromides with aryl triflates. *Nature* **524**, 454–457 (2015).

3. Qiu, Z. & Li, C.-J. Transformations of less-activated phenols and phenol derivatives via C–O cleavage. *Chem. Rev.* **120**, 10454–10515 (2020).

4. Wong, S. S., Shu, R., Zhang, J., Liu, H. & Yan, N. Downstream processing of lignin derived feedstock into end products. *Chem. Soc. Rev.* **49**, 5510–5560 (2020).

5. Zhang, Y. *et al.* Recent advances in Rochow-Müller process research: driving to molecular catalysis and to a more sustainable silicone industry. *ChemCatChem* **11**, 2757–2779 (2019).

6. Finholt, A. E., Bond, A. C., Wilzbach, K. E. & Schlesinger, H. I. The preparation and some properties of hydrides of elements of the fourth group of the periodic system and of their organic derivatives. *J. Am. Chem. Soc.* **69**, 2692–2696 (1947).

7. Toutov, A. A. *et al.* Silylation of C–H bonds in aromatic heterocycles by an earth-abundant metal catalyst. *Nature* **518**, 80–84 (2015).

8. Kan, S. B. J., Lewis, R. D., Chen, K. & Arnold, F. H. Directed evolution of cytochrome c for carbon–silicon bond formation: bringing silicon to life. *Science* **354**, 1048–1051 (2016).

9. Sun, K. *et al.* On-surface synthesis of disilabenzene-bridged covalent organic frameworks. *Nat. Chem.* **15**, 136–142 (2023).

10. Liu, Y., Stringfellow, T. C., Ballweg, D., Guzei, I. A. & West, R. Structure and chemistry of 1-silafluorenyl dianion, its derivatives, and an organosilicon diradical dianion. *J. Am. Chem. Soc.* **124**, 49–57 (2002).

11. Showell, G. A. & Mills, J. S. Chemistry challenges in lead optimization: silicon isosteres in drug discovery. *Drug Discov. Today* **8**, 551–556 (2003).

12. Franz, A. K. & Wilson, S. O. Organosilicon molecules with medicinal applications. *J. Med. Chem.* **56**, 388–405 (2013).

13. Hatanaka, Y. & Hiyama, T. Cross-coupling of organosilanes with organic halides mediated by a palladium catalyst and tris(diethylamino)sulfonium difluorotrimethylsilicate. *J. Org. Chem.* **53**, 918–920 (1988).

14. Nakao, Y. & Hiyama, T. Silicon-based cross-coupling reaction: an environmentally benign version. *Chem. Soc. Rev.* **40**, 4893–4901 (2011).

15. De Meio, G., Morgan, J. & Pinhey, J. T. Aryl fluoride syntheses involving reaction of aryllead triacetates with boron trifluoride-diethyl ether complex. *Tetrahedron* **49**, 8129–8138 (1993).

16. Wilson, S. R. & Jacob, L. A. Iodination of aryltrimethylsilanes. A mild approach to (iodophenyl)alanine. *J. Org. Chem.* **51**, 4833–4836 (1986).

17. Sakurai, H., Hosomi, A. and Kumada, M. Addition of trichloromethyl radicals to alkenylsilanes. *J. Org. Chem.* **34**, 1764–1768 (1969).

18. Hosomi, A. Characteristics in the reactions of allylsilanes and their applications to versatile synthetic equivalents. *Acc. Chem. Res.* **21**, 200–206 (1988).

19. Tobisu, M. & Chatani, N. Cross-couplings using aryl ethers via C–O bond activation enabled by nickel catalysts. *Acc. Chem. Res.* **48**, 1717–1726 (2015).

20. Cornella, J., Zarate, C. & Martin, R. Metal-catalyzed activation of ethers via C–O bond cleavage: a new strategy for molecular diversity. *Chem. Soc. Rev.* **43**, 8081–8097 (2014).

21. Zarate, C., Nakajima, M. & Martin, R. A mild and ligand-free Ni-catalyzed silylation via C–OMe cleavage. *J. Am. Chem. Soc.* **139**, 1191–1197 (2017).

22. Cao, Z.-C. & Shi, Z.-J. Deoxygenation of ethers to form carbon–carbon bonds via nickel catalysis. *J. Am. Chem. Soc.* **139**, 6546–6549 (2017).

23. Nakamura, K., Tobisu, M. & Chatani, N. Nickel-catalyzed formal homocoupling of methoxyarenes for the synthesis of symmetrical biaryls via C–O bond cleavage. *Org. Lett.* **17**, 6142–6145 (2015).

24. Rawat, V. K., Higashida, K. & Sawamura, M. Nickel-catalyzed homocoupling of aryl ethers with magnesium anthracene reductant. *Synthesis* **53**, 3397–3403 (2021).

25. Tang, J. *et al.* Chemoselective cross-coupling between two different and unactivated C(aryl)–O bonds enabled by chromium catalysis. *J. Am. Chem. Soc.* **142**, 7715–7720 (2020).

26. Zarate, C., van Gemmeren, M., Somerville, R. J. & Martin, R. Chapter Four – phenol derivatives: modern electrophiles in cross-coupling reactions. *Adv. Organomet. Chem.* **66**, 143–222 (2016).

27. Duan, J. *et al.* Cross-electrophile C(sp^2)−Si coupling of vinyl chlorosilanes. *Angew. Chem. Int. Ed.* **59**, 23083–23088 (2020).

28. Zhao, Z.-Z., Pang, X., Wei, X.-X., Liu, X.-Y. & Shu, X.-Z. Nickel-catalyzed reductive C(sp^2)−Si coupling of chlorohydrosilanes via Si−Cl cleavage. *Angew. Chem. Int. Ed.* **61**, e202200215 (2022).

29. Seki, R., Hara, N., Saito, T. & Nakao, Y. Selective C–O bond reduction and borylation of aryl ethers catalyzed by a rhodium–aluminum heterobimetallic complex. *J. Am. Chem. Soc.* **143**, 6388–6394 (2021).

30. The geometry optimization was performed by the DFT method with B3LYP/6-31+g(d) level of theory. The natural populations were calculated by NBO7.

31. Miura, H. *et al.* Diverse alkyl–silyl cross-coupling via homolysis of unactivated C(sp^3)–O bonds with the cooperation of gold nanoparticles and amphoteric zirconium oxides. *J. Am. Chem. Soc.* **145**, 4613–4625 (2023).

32. Lim, S. *et al.* Cobalt-catalyzed defluorosilylation of aryl fluorides via Grignard reagent formation. *Org. Lett.* **22**, 7387–7392 (2020).

33. Kusumoto, S. & Nozaki, K. Direct and selective hydrogenolysis of arenols and aryl methyl ethers. *Nat. Commun.* **6**, 6296–6302 (2015).

34. Jin, X. *et al.* Metal–support cooperation in $Al(PO_3)_3$-supported platinum nanoparticles for the selective hydrogenolysis of phenols to arenes. *Nat. Catal.* **4**, 312–321 (2021).

35. Aleandri, L. E. *et al.* Inorganic Grignard reagents. Preparation and their application for the synthesis of highly active metals, intermetallics, and alloys. *Chem. Mater.* **7**, 1153–1170 (1995).

36. Iwasaki, T. *et al.* Diarylrhodates as promising active catalysts for the arylation of vinyl ethers with Grignard reagents. *J. Am. Chem. Soc.* **136**, 9260–9263 (2014).

37. Bogdanović, B., Leitner, W., Six, C., Wilczok, U. & Wittmann, K. “Grignard-analogous” rhodium phosphane complexes. *Angew. Chem. Int. Ed.* **36**, 502–504 (1997).

38. Pietrasiak, E. *et al.* Cobalt-catalyzed formation of Grignard reagents via C–O or C–S bond activation. *J. Org. Chem.* **87**, 8380–8389 (2022).

39 . Sawano, T. *et al.* The first chiral diene-based metal-organic frameworks for highly enantioselective carbon–carbon bond formation reactions. *Chem. Sci.* **6**, 7163–7168 (2015).

40. Kirchhof, M. *et al.* Experimental and theoretical study on the role of monomeric vs dimeric rhodium oxazolidinone norbornadiene complexes in catalytic asymmetric 1,2- and 1,4-additions. *Organometallics* **39**, 3131–3145 (2020).

41. Hayashi, T., Takahashi, M., Takaya, Y. & Ogasawara, M. Catalytic cycle of rhodium-catalyzed asymmetric 1,4-addition of organoboronic acids. Arylrhodium, oxa-π-allylrhodium, and hydroxorhodium intermediates. *J. Am. Chem. Soc.* **124**, 5052–5058 (2002).

42. Xue, W., Shishido, R. & Oestreich, M. Bench-stable stock solutions of silicon Grignard reagents: application to iron- and cobalt-catalyzed radical C(sp^3)–Si cross-coupling reactions. *Angew. Chem. Int. Ed.* **57**, 12141–12145 (2018).